PROCEEDINGS OF SCIENCE

Study of cosmic ray propagation using GALPROP

Hongyi Wu[1]
Univ. of Maryland College Park
Inst. for Phys. Sci. and Tech., University of Maryland, College Park, MD 20742, USA
E-mail: hwu1@terpmail.umd.edu

Eun-Suk Seo
Univ. of Maryland College Park
Inst. for Phys. Sci. and Tech., University of Maryland, College Park, MD 20742, USA
E-mail: seo@umd.edu

Vladimir Ptuskin
IZMIRAN, Moscow
IZMIRAN, Troitsk, Moscow 108840, Russia
E-mail: vptuskin@hotmail.com

Significant spectral hardening at around 200 GV magnetic rigidity has been reported by AMS-02, ATIC-2, CALET, CREAM, DAMPE, and PAMELA. This has been observed in high-accuracy measurements of various nuclei energy spectra of both primaries and secondaries. To explain the spectral hardening while maintaining proper B/C and p/He ratios, we study 3 approaches in a reacceleration model: adding a diffusion coefficient break, introducing extra source injection breaks, and a combination of both. We use the numerical code GALPROP to compute the propagation of cosmic rays with such parameter sets on the rigidity dependence of source and propagation parameters. Implications on the positron spectra are discussed.

37th International Cosmic Ray Conference (ICRC 2021)
July 12th – 23rd, 2021
Online – Berlin, Germany

[1]Presenter, undergraduate student

1. Introduction

Recent high-accuracy measurements of cosmic ray energy spectra have revealed spectral deviation from a single power law. The presence of spectral hardening was found in calorimeter-based experiments ATIC-2[1] and CREAM[2] on balloons and DAMPE[3] and CALET[4] in space, and magnetic spectrometer experiments PAMELA[5] and AMS[6]. The origin of this phenomenon is still uncertain and may reflect the corresponding breaks of the source spectra and/or the diffusion coefficient. It could also be an effect of new cosmic ray sources. In this paper we present 3 cases with breaks in (1) the diffusion coefficient, (2) the source spectra and, (3) a combination of both. The results are compared with data from various experiments on cosmic ray p, p-, e-, e+; He, Li, Be, B, C, O, Ne, Mg, Si, and Fe nuclei.

2. Model

We use GALPROP[7] numerical code to calculate the propagation of relativistic charged particles. It contains diffusive reacceleration and nuclear spallation, secondary particle production, radioactive decay, electron interactions, and so on. Equation 1 is the main equation GALPROP solves numerically.

Sources
including primary, spallation and decay contributions

Diffusion
Dxx: spatial diffusion coefficient

Fragmentation
τ_f: time

$$\frac{\partial \psi(\vec{r},p,t)}{\partial t} = q(\vec{r},p,t) + \vec{\nabla}\cdot(D_{xx}\vec{\nabla}\psi - \vec{V}\psi) + \frac{\partial}{\partial p}p^2 D_{pp}\frac{\partial}{\partial p}\frac{1}{p^2}\psi - \frac{\partial}{\partial p}\left[\dot{p}\psi - \frac{p}{3}(\vec{\nabla}\cdot\vec{V})\psi\right] - \frac{1}{\tau_f}\psi - \frac{1}{\tau_r}\psi \quad (1)$$

CR density per unit

Diffusive reacceleration

Energy loss
ṗ: Momentum

Decay
τ_r: time

GALPROP provides one rigidity break where the diffusion coefficient index can be different above and below it. The diffusion coefficient relates to rigidity in the form $D \propto \beta D_{0xx} R^{-D_g}$, where β is *v*/c, D_{0xx} is the normalized diffusion coefficient, D_rigid_br is the break rigidity, D_g is the diffusion coefficient index. The source spectra also pose a power-law relation to rigidity in the form: $\Phi \propto R^{-\gamma}$, where R is the rigidity and γ is the injection index. Similar to how GALPROP handles the diffusion coefficient, we can add several rigidity breaks in the computation with different injection indices above and below them. The p flux and e- flux are normalized at a kinetic energy of 100 GeV per nucleon. The heavy nuclei (Z > 2) fluxes are also normalized according to the relative abundances. We consider diffusion models with a static cosmic ray halo size H = 4 kpc.

In this study, we use GALPROP to calculate the cosmic ray propagation to fit the measured B/C ratio, p/He ratio, nuclei spectra, etc.

3. Methods and Verification

We use GALPROP version 56 with default parameters from the plain diffusion model in GALPROP WebRun (version 54).[7] The default model has a break in the diffusion coefficient and no second breaks in the source spectra.

According to the AMS data, the spectra of p-, Li, Be, B, C, and O all show a significant hardening at high energies, starting at ~ 200 GV in rigidity. We consider three cases to fit the hardening and find a case preferred by data.[8,9,10,11,12]

Case 1 includes only a diffusion coefficient break. We add a break at 300 GV to have the diffusion coefficient index changes from 0.514 to 0.27 as shown in the blue cells in Table 1.

Case 2 includes only source breaks. We apply different source changes to different elements. The injection index changes from 2.350 to 2.035 at 500 GV for p, from 2.274 to 2.039 at 300 GV for He, from 2.364 to 2.06 at 300 GV for heavy nuclei (Z > 2), and from 2.725 to 2.520 at 1000 GV for e-, as shown in the orange cells in Table 1.

Case 3 includes both diffusion coefficient and source breaks. The diffusion coefficient index changes from 0.514 to 0.40 at 200 GV. The injection index changes from 2.330 to 2.18 at 800 GV for p, from 2.274 to 2.099 at 400 GV for He, from 2.364 to 2.18 at 250 GV for heavy nuclei (Z > 2), and from 2.725 to 2.620 at 1000 GV for e-, as shown in the green cells in Table 1.

Table 1. GALPROP parameters for the three cases: *Case 1 (diffusion break), Case 2 (source breaks) and Case 3 (diffusion and source breaks).*

Item		Case 1	Case 2	Case 3
The Alfven speed	v_{Alfven} (km·s^{-1})	7.64	7.64	7.64
Diffusion coefficient: $D \propto \beta D_{0xx} R^{-D_g}$	D_{0xx} (10^{29}cm^{2}s^{-1})	3.0	2.5	3.25
	D_{g1}	0.514	0.51	0.514
	R (GV)	300	-	200
	D_{g2}	0.27	-	0.40
Proton source injection: $\Phi \propto R^{-\gamma}$	γ_1	1.84	1.84	1.84
	R_1 (GV)	5.78	5.78	5.78
	γ_2	2.350	2.350	2.330
	R_2 (GV)	-	500	800
	γ_3	-	2.035	2.18
Helium source injection: $\Phi \propto R^{-\gamma}$	γ_1	1.344	1.644	1.644
	R_1 (GV)	5.78	5.78	5.78
	γ_2	2.3	2.274	2.274
	R_2 (GV)	-	300	400
	γ_3	-	2.039	2.099
Heavy nuclei with Z>2 source injection: $\Phi \propto R^{-\gamma}$	γ_1	1.864	1.864	1.864
	R_1 (GV)	5.78	5.78	5.78
	γ_2	2.364	2.364	2.364
	R_2 (GV)	-	300	250
	γ_3	-	2.06	2.18
Electron source injection: $\Phi \propto R^{-\gamma}$	γ_1	1.63	1.63	1.63
	R_1 (GV)	5.78	5.78	5.78
	γ_2	2.725	2.725	2.725
	R_2 (GV)	-	1000	1000
	γ_3	-	2.520	2.620

The source abundance settings are identical in all three cases, as shown in Table 2. A primary Li source is considered in all three cases. A comparison of the Li spectrum with and without the primary Li source is shown in Section 4.

Table 2. Primary source abundance settings (including primary Lithium)

Nuclei	Source abundance	Nuclei	Source abundance	Nuclei	Source abundance
^{1}H	$1.06*10^{6}$	^{12}O	4106.8	^{28}Si	726.52
^{4}He	95525.52	^{20}Ne	477.36	^{54}Fe	36.08
^{12}C	3154.92	^{24}Mg	622.64	^{7}Li	65.00

4. Data and Discussion

Our results on the B/C ratio and the p/He ratio for the three different parameter sets are shown in Figure 1. All three cases give reasonable fits to data. Minor differences in the B/C ratio at high energies are resulted from diffusion coefficient break settings. The high energy B/C ratio is directly influenced by the diffusion coefficient index.

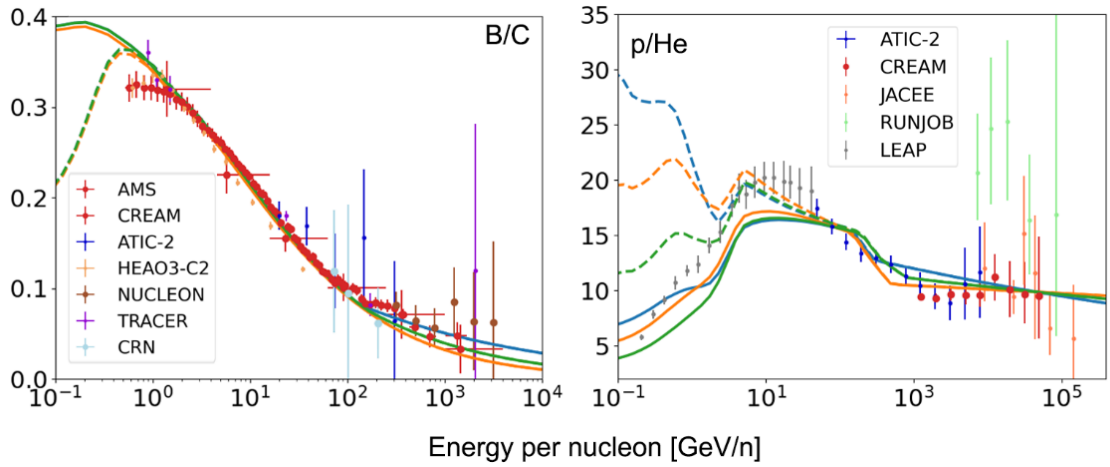

Figure 1. The B/C (left) and p/He (right) ratios produced by GALPROP v56. Solid curves represent our Galprop results with solar modulation 610 MV, and dashed curves represent interstellar ratios. Case 1, Case 2, and Case 3 are shown as blue, orange, and green curves.

Figure 2 shows the p, p-, O, He, C, B, Li, and Be spectra. The diffusion-coefficient break-rigidity calculated for the B/C ratio results in a break lower than the observed break in the p spectrum and higher than that in the p- spectrum. Besides, the diffusion coefficient index in Case 1 that produces enough hardening in the p and He spectra does not produce enough hardening in the C and O spectra. The source injection break in Case 2 that produces hardening in p, C and O spectra does not produce enough hardening in the B and Be spectra. Although not shown here, our results of the Ne, Mg, Si, and Fe spectra are in a reasonable agreement with the data.

Figure 3 shows the comparison of Li spectrum with (right) and without (left) a primary Li source for the three cases. The pure secondary Li from GALPROP cannot produce the Li observed in the data as shown in Figure 3 (left).[13] By adding a Li source injection spectrum GALPROP produces Li in agreement with the data as shown in Figure 3 (right). The Li source injection spectrum is the same as that of the heavy nuclei (Z > 2).

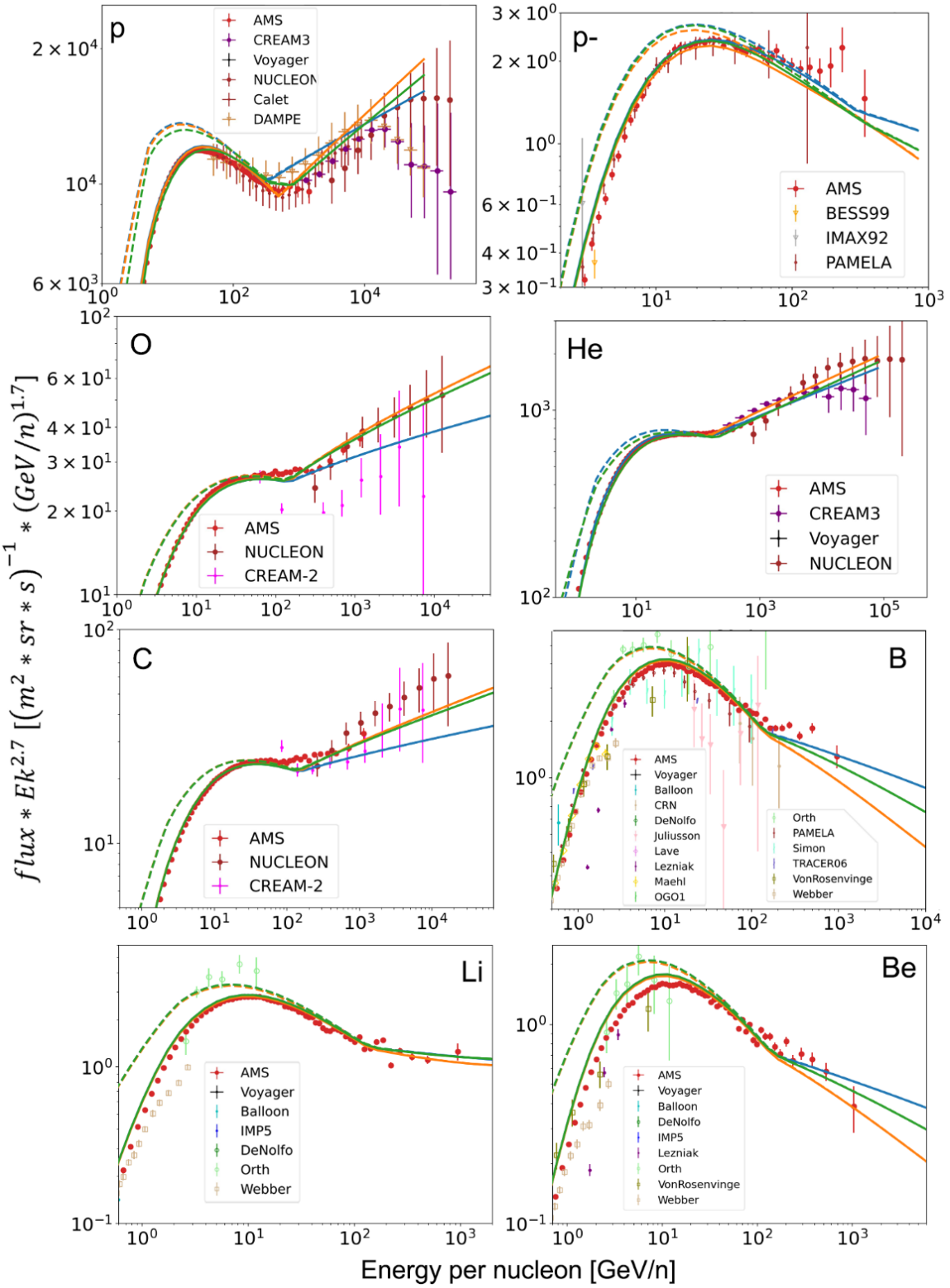

Figure 2. Elemental spectra produced by GALPROP v56. Solid curves represent our Galprop results with solar modulation 610 MV, and dashed curves represent interstellar spectra. Case 1, Case 2, and Case 3 are shown as blue, orange, and green curves.

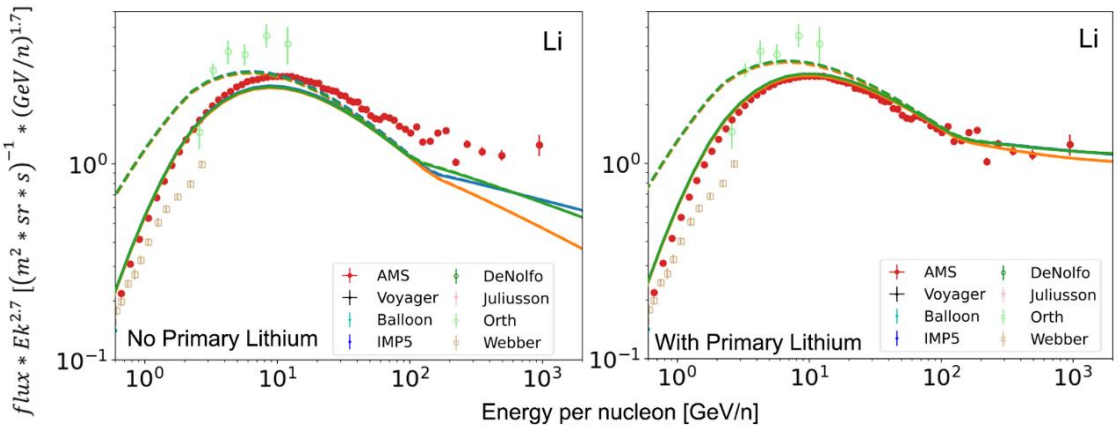

Figure 3. The Li spectrum without a primary Li source (left) and Li spectrum with a primary Li source (right) produced by GALPROP v56. Solid curves represent our Galprop results with solar modulation 610 MV, and dashed curves represent interstellar spectra. Case 1, Case 2, and Case 3 are shown as blue, orange, and green curves.

Figure 4 shows the e- (left) and e+ (right) spectra compared with the data. All three cases produce almost identical results in both e- and e+ spectra. They are in an acceptable agreement with e- data, but there is a significant disagreement with e+ data.

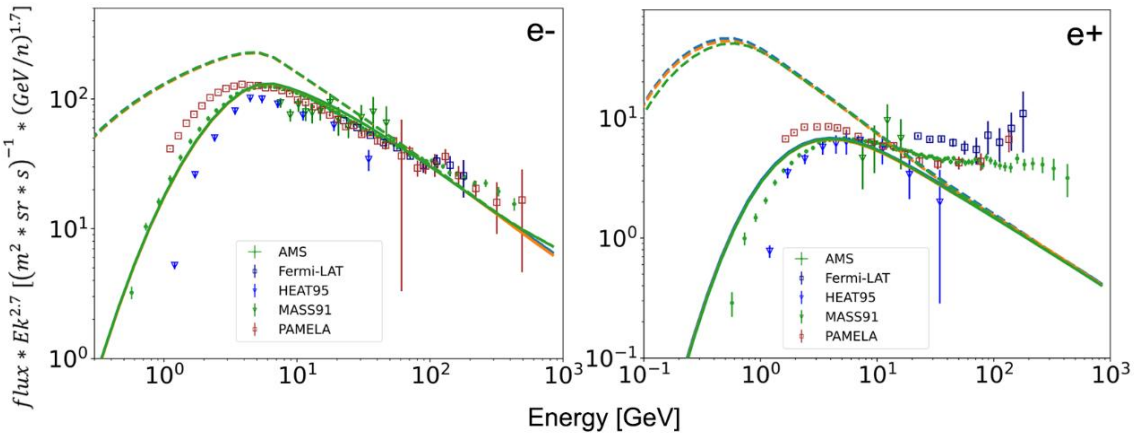

Figure 4. The e- (left) and e+ (right) spectra produced by GALPROP v56. Solid curves represent our Galprop results with solar modulation 610 MV, and dashed curves represent interstellar spectra. Case 1, Case 2, and Case 3 are shown as blue, orange, and green curves.

To study this discrepancy, the GALPROP output is subtracted from the AMS e+ data. Case 3 with modulation 610 MV is used. The difference between the GALPROP result and data is shown in Figure 5. We made a power-law fit to the subtracted data points. The fitting function is given by $flux_{e+} = A * E^{\alpha - 2.7} + B * E^{-2.7}$, where E is the energy and A, B, α are constants. The calculation yields A = -11.51, B = 5.45, α = -0.286.

A possibility of an extra e+ source is investigated using a primary e+ source given by:

$$\Phi \propto R^{-\gamma}, \begin{cases} \gamma = 1.83, for\ R \leq 5.78\ GV \\ \gamma = 2.5, for\ 5.78\ GV \leq R < 30\ GV \\ \gamma = 2.05, for\ R > 30\ GV \end{cases} \quad (2)$$

In this Case 4, the diffusion coefficient is the same as Case 3 given in Table 1. The calculated e+ spectrum is presented in Figure 6. The result with modulation 610 MV is the solid purple curve and the interstellar result is the dashed purple curve. As Figure 6 shows, this primary e+ source can generate the e+ spectrum with consistency to data, showing significant improvement from the secondary e+ generated in the previous three cases. The calculated spectrum indicates that the diffusion coefficient break at 200 GV does not have a significant impact on the e+ flux.

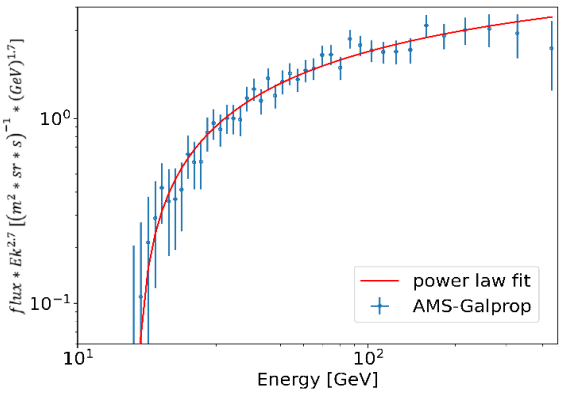

Figure 5. The e+ flux difference between AMS data and the Galprop output for case 3. The power-law fit is shown as the red curve.

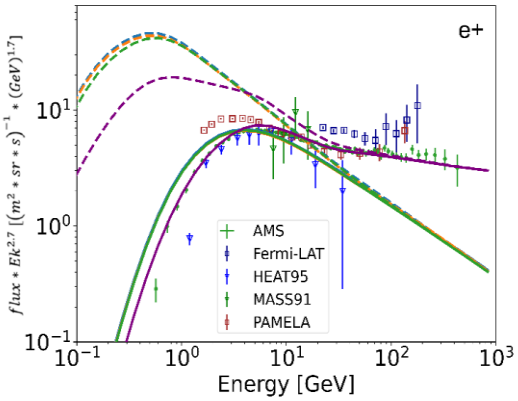

Figure 6. The e+ spectrum produced by GALPROP v56. Solid curves represent our Galprop results with solar modulation 610 MV, and dashed curves represent interstellar spectra. Case 1, Case 2, Case 3, Case 4 are shown as blue, orange, green, and purple curves.

5. Conclusion

By adding a diffusion coefficient break at 300 GV where the index changes from 0.514 to 0.27, GALPROP produces acceptable B/C ratio. But it results in a break lower than the observed break in the p spectrum and higher than that in the p- spectrum. The resulting spectral hardening agrees with the p and He data but is not sufficient to fit the C and O data.

By changing the injection index from 2.350 to 2.035 at 500 GV for p, from 2.274 to 2.039 at 300 GV for He, and from 2.364 to 2.06 at 300 GV for heavy nuclei (Z > 2), GALPROP produces spectral hardening in agreement with all the primary cosmic ray data including C and O. But the resulting spectral hardening is not sufficient to fit the B and Be data.

By having both diffusion coefficient and source injection breaks, GALPROP produces the spectral hardening in agreement with data simultaneously. The diffusion coefficient index changes from 0.514 to 0.40 at 200 GV, and the injection index changes from 2.330 to 2.18 at 800 GV for p, from 2.274 to 2.099 at 400 GV for He, and from 2.364 to 2.18 at 250 GV for heavy nuclei (Z > 2).

We also examined if the spectral hardening supports the existence of a primary Li source and calculated the relative abundance. The Li source with the same source injection as the heavy nuclei (Z > 2) and an abundance of 65 (relative to the p source abundance $1.06*10^6$) greatly improves the consistency of GALPROP results with data.

The hardening in the e+ spectrum cannot be explained with all three cases we studied but can be fitted by adding a primary e+ source. This e+ source has a rigidity break at 30 GV at which the injection index changes from 2.5 to 2.05.

References

[1] A.D. Panov, et al. *Elemental energy spectra of cosmic rays from the data of the ATIC-2 experiment*, Bull.Rus.Acad. Sci. Phys, **71** (2007), 494.

[2] H.S. Ahn, et al. *Discrepant hardening observed in cosmic-ray elemental spectra*, Astrophys. J. Lett, **714** (2010), L89.

[3] Q. An, et al. *Measurement of the Cosmic Ray Proton Spectrum from 40 GeV to 100 TeV with the DAMPE Satellite.* Science Advances **5/9** (2019).

[4] O. Adriani, et al. *Direct Measurement of the Cosmic-Ray Proton Spectrum from 50 GeV to 10 TeV with the Calorimetric Electron Telescope on the International Space Station.* Phys. Rev. Lett. **122/18** (2019).

[5] O. Adriani, et al. *PAMELA Measurements of Cosmic-Ray Proton and Helium Spectra*, Science, **332** (2011), 69.

[6] H. S. Ahn, et al. *Measurements of cosmic-ray secondary nuclei at high energies with the first flight of the CREAM balloon-borne experiment.* Astroparticle Physics **30** (2008), 133–141.

[7] https://galprop.stanford.edu/webrun/

[8] A. D. Panov, et al. *The Results of ATIC-2 Experiment for Elemental Spectra of Cosmic Rays.* Bull. Russ. Acad. Sci. Phys. **71** (2007), 494-497.

[9] V. Grebenyuk, et al. *Energy Spectra of Abundant Cosmic-Ray Nuclei in the NUCLEON Experiment.* Advances in Space Research, **64/12** (2019).

[10] Y. S. Yoon, et al. *Proton and Helium Spectra from the CREAM-III Flight*. Astrophys. J., **839/5** (2017).

[11] A. C. Cummings, et al. *Galactic Cosmic Rays In The Local Interstellar Medium: Voyager 1observations And Model Results*. Astrophys. J. **831/1** (2016), 18.

[12] E. S. Seo, *Advances in Direct Measurements of Cosmic Rays.* J. Korean Phys. Soc. **78/10** (2021), 923.

[13] M. J. Boschini, et al. *Deciphering the Local Interstellar Spectra of Secondary Nuclei with GALPROP/HelMod Framework and a Hint for Primary Lithium in Cosmic Rays*. Astrophys. J. **2** (2020): 167